Sustainable Food Technology

ROYAL SOCIETY OF CHEMISTRY

PAPER

View Article Online
View Journal

Cite this: DOI: 10.1039/d5fb00787a

Unveiling the effects of cold plasma treatment on the structural, rheological, and functional properties of rice bean protein isolate

Charu Agarwal,[a] Rachna Sehrawat,[b] Loveleen Sharma *[a] and Manoj Kumar Patel *[cd]

In the present study, the impact of cold plasma treatment (CPT) on rice bean protein isolate (RBPI) was systematically investigated to evaluate its functional and structural modifications. Unlike previous CPT studies, which primarily focused on soy, pea, or wheat proteins, this work explores rice bean protein—a nutritionally rich but underutilized legume source—with the aim of enhancing its techno-functional qualities for food applications. The untreated RBPI (sample A) was subjected to CPT under varied treatment intensities, and the optimal condition was identified based on the greatest improvement across multiple functional and structural parameters. Notably, sample F (20 kV for 10 minutes) exhibited the most significant enhancements. Among all treatments, the optimally modified sample exhibited major improvements, including increases in protein solubility from 71.95% to 88.13%, foaming capacity from 33.3% to 300%, emulsifying activity from 30% to 58%, and water-binding capacity from 2.09 g g^{-1} to 2.94 g g^{-1}. Scanning electron microscopy (SEM) showed greater surface porosity and particle fragmentation, while Fourier transform infrared (FTIR) spectroscopy confirmed alterations in secondary structure, particularly enhanced β-sheet content. Rheological analysis demonstrated improved viscoelasticity and gel strength, and SDS-PAGE verified that CPT altered conformation without affecting molecular integrity. ANOVA and DMRT statistical analysis revealed significant improvements ($p < 0.01$) in both functional and structural attributes in the treated samples compared to the untreated ones. Collectively, these results underscore the potential of cold plasma treatment as a viable approach for improving the structural and functional properties of rice bean protein isolate.

Received 30th October 2025
Accepted 1st December 2025

DOI: 10.1039/d5fb00787a

rsc.li/susfoodtech

Sustainability spotlight

This study advances sustainable food processing by employing cold plasma, a non-thermal, energy-efficient, and chemical-free technology, to enhance the structural, functional, and rheological properties of rice bean protein isolate. Utilizing rice bean—a climate-resilient, underexploited legume—promotes biodiversity, reduces reliance on major protein crops, and supports nutritional security. The plasma-based modification approach minimizes the uses of water and chemical, aligning with the principles of green processing and circular bioeconomy. This work contributes directly to the UN Sustainable Development Goals by fostering resource-efficient food innovation (SDG 12), enhancing access to sustainable protein sources (SDG 2), and mitigating environmental impact through the uses of low-carbon processing technologies (SDG 13).

1. Introduction

Rice bean (*Vigna umbellata*) is a protein-rich legume belonging to the Vigna genus, which includes mung bean (*Vigna radiata*), adzuki bean (*Vigna angularis*), and black gram (*Vigna mungo*). It contains a high concentration of essential amino acids, including methionine, tryptophan, lysine, tyrosine, and valine, with a total protein content ranging from 14–24%, of which approximately 60% is digestible. It is noted to be very rich in protein, minerals, and vitamins.[1,2] It is mainly used for human dietary uptake, with a smaller proportion used for fodder and green manuring. It is believed to have been domesticated in the Myanmar–Thailand region, and it carries social and cultural values in some communities in India, where it is confined to the Northeastern hills, Western and Eastern Ghats, and parts of Himachal Pradesh. Rice bean is resistant to storage pests and can be successfully cultivated in comparatively poor soils under high temperatures and low rainfall conditions.[3–5] Despite its

[a]Amity Institute of Food Technology, Amity University, Noida-201313, Uttar Pradesh, India. E-mail: sharmaloveleen88@gmail.com; lsharma8@amity.edu

[b]Department of Food Process Engineering, National Institute of Technology, Rourkela, Odisha, 769008, India

[c]CSIR – Central Scientific Instruments Organisation, Chandigarh-160030, India. E-mail: manoj_patel.csio@csir.res.in; patelnitjsr@gmail.com

[d]Academy of Scientific and Innovative Research, Ghaziabad-201002, Uttar Pradesh, India

nutritional potential, its techno-functional and structural properties remain underexplored, and only limited studies have addressed its behaviour as a functional ingredient in food systems.[6,7]

Proteins from plant sources often suffer from poor solubility, low digestibility, and limited functionality in food systems.[8,9] These limitations are often attributed to their compact structure, low surface hydrophobicity, and rigid secondary conformations. Modifying the protein structure, particularly through techniques that promote structural unfolding or controlled aggregation, can enhance these properties. Among various emerging technologies, non-thermal processing methods such as ultrasound, high-pressure treatment, and pulsed electric fields have shown promise in altering protein conformations without compromising nutritional quality.[10–13]

The Cold Plasma Treatment (CPT) is a non-thermal technique that can be a viable alternative for preserving nutritional quality compared to other traditional methods.[14–16] In general, plasma is generated by increasing the energy level of gas to achieve the ionised state, which contains several active species, such as electrons, free radicals, ions, reactive oxygen, and nitrogen species.[17] Furthermore, generated plasma is partially ionised at low temperatures (<60 °C), and reaching the equilibrium condition indicates the formation of cold plasma.[18] During CPT, reactive species interact with macromolecules, promoting the cross-linking, depolymerisation, surface etching, oxidation, hydroxylation, nitration, sulfonation, sulfoxidation, and amidation processes.[19] Several studies have demonstrated that CPT enhances the functional properties of different plant proteins, including sunflower, peanut, whey, and mung bean proteins.[20–23] These studies collectively demonstrate that CPT can modify protein conformation, enhance interfacial properties, and alter secondary structures, particularly shifting α-helix and random coil content toward β-sheet and β-turn structures.[24,25]

However, despite extensive research on other plant proteins, no published studies have investigated the impact of CPT on rice bean protein isolate (RBPI). Given the nutritional value of rice bean and its potential as a functional ingredient, there is a critical need to understand how CPT can be used to tailor its structural and functional attributes.

The present study investigates the physicochemical, functional, and structural properties of rice bean protein isolate modified at different CPT conditions. While previous studies have explored CPT effects on pea, chickpea, walnut, soy, quinoa, hemp, sunflower and mung bean proteins,[12,20,26–29] no reports are available on the CPT of RBPI, despite its considerable nutritional potential. The present work addresses this gap by examining how cold plasma exposure influences the structural organisation and functional performance of rice bean protein isolate. The study focuses on the extent to which different plasma intensities alter the protein's conformation, surface characteristics and techno-functional attributes, with particular emphasis on solubility, emulsifying behaviour, foaming capacity and water-binding ability. Through this approach, the investigation aims to identify treatment conditions that most effectively enhance the usability of rice bean protein as a functional food ingredient and to establish CPT as a promising, clean-label strategy for improving the application potential of this underutilised plant protein.

2. Materials and methods

The rice beans used for the research were procured from the local market of Manipur, India, where they are locally known as Chakhwai. The beans were manually cleaned to remove stones, dust, and foreign matter, and subsequently ground into flour using a laboratory flour mill (Food Processing Lab, Amity University, Noida, Uttar Pradesh, India). All chemicals and reagents used in the study were of analytical grade and were purchased from HiMedia Laboratories Pvt. Ltd (Mumbai, India). Bovine serum albumin (BSA), used as the standard for protein quantification, was obtained from Sigma-Aldrich (Germany). Deionized water used in all experiments was produced using a Milli-Q purification system (Millipore, USA). Cold plasma treatment was carried out using the CPT unit installed at NIT Rourkela, India (0.23 kV, 50 Hz, IN-HVLT MP, Ingenium Naturae Pvt. Ltd, Gujarat, India). The system consisted of a multipin electrode array and operated using ambient air as the feed gas. All experiments were conducted at room temperature, and the discharge parameters were maintained as per the operational specifications of the equipment.

2.1. Isolation of protein from rice bean flour

The protein was isolated from rice bean flour using the alkali–acid extraction method with slight modifications.[30] The rice bean flour was mixed with distilled water at a 1 : 10 meal to solvent ratio. The pH of the mixture was adjusted to 11 by using 2 N NaOH and stirred for 1 hour. The mixture was then centrifuged (8000 rpm for 20 minutes), and the supernatant was collected. Then the pH of the supernatant was adjusted to pH 4.5 using 0.2 N HCl and was left for 30 minutes to achieve complete protein precipitation. After 30 minutes, the solution was centrifuged (8000 rpm for 20 minutes), the supernatant was discarded, and the precipitated proteins were collected and freeze-dried. The isolated rice bean protein isolate exhibited a protein content of 92.4%, as determined using the Kjeldahl method.

2.2. Cold plasma treatment

Cold plasma treatment was carried out using an atmospheric cold plasma (ACP) system equipped with a multipin electrode configuration comprising stainless steel pins, covering a discharge area of 18.5 × 25 cm^2. The schematic diagram of CPT on RBPI is shown in Fig. 1. The system operates at an alternating current (AC) high-voltage power supply, with the applied voltages adjusted to 10 kV and 20 kV, depending on the treatment condition. The plasma discharge was generated in ambient air, which served as the feed gas, containing natural mixtures of nitrogen, oxygen, and trace humidity. This composition generates reactive oxygen and nitrogen species (ROS and RNS), which are responsible for protein surface modification.[31] The isolated rice bean protein sample was used

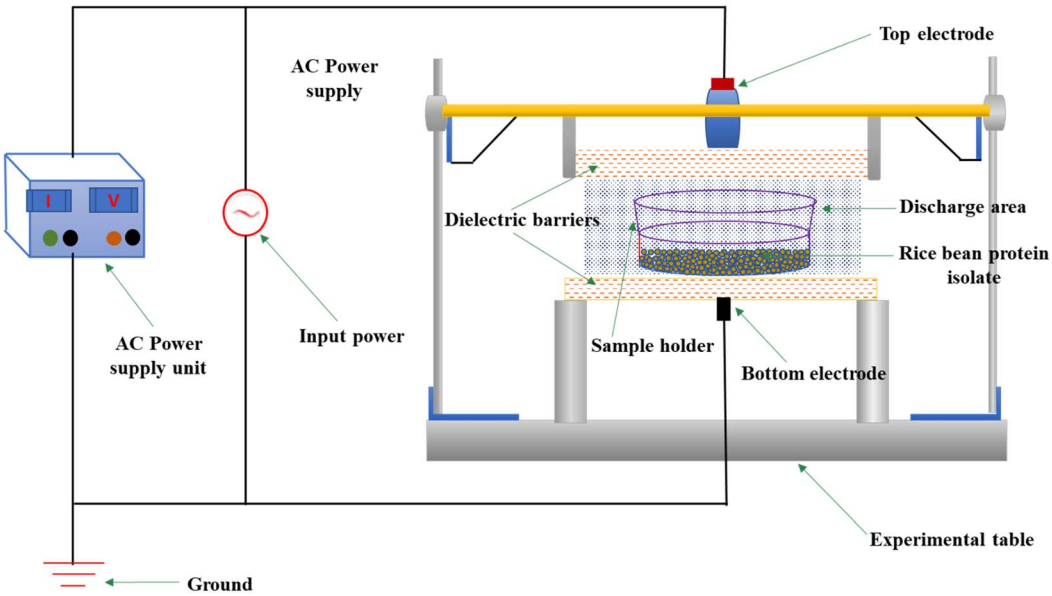

Fig. 1 Schematic diagram of cold plasma treatment of rice bean protein isolate.

in powdered form, uniformly spread on 90 mm Petri plates, maintaining a consistent sample thickness of 2.0–2.5 mm. The powdered state was chosen to maximize the surface area exposed to reactive plasma species, ensure uniform discharge interaction, and prevent localized overheating or uneven modification that can occur in moist or slurry forms. Additionally, the powdered form allows consistent control of electrode distance and sample geometry, ensuring reproducible plasma exposure and minimizing variability in treatment effects.

The electrode gap was maintained at a fixed distance of 7 cm for all experiments, and all treatments were conducted at room temperature (approximately 25 °C). Based on preliminary trials, the treatment duration was optimized between 5 and 20 minutes, as this range produced the most effective physicochemical changes without causing excessive protein denaturation.

Treatments were carried out under the following conditions: untreated (A), 10 kV for 5 minutes (B), 10 kV for 10 minutes (C), 10 kV for 20 minutes (D), 20 kV for 5 minutes (E), 20 kV for 10 minutes (F), and 20 kV for 20 minutes (G).

2.3. Functional properties

2.3.1. Solubility. The solubility of untreated RBPI and cold plasma-treated samples was measured using the methodology described by Li and co-authors.[32] RBPI solutions were centrifuged at 3000 rpm for 15 minutes, and the supernatant was collected. Their protein concentration was measured using the Lowry assay method.[33] Bovine serum albumin (BSA) (Sigma-Aldrich, Germany) was used as the standard, with concentrations ranging from 0 to 10 mg mL^{-1} at 2 mg mL^{-1} intervals. Absorbance was recorded at 750 nm using a UV-visible spectrophotometer. The ratio of the soluble protein in the supernatant to the total protein in the dispersion represents the relative solubility (%) of protein.

2.3.2. Wettability. A 250 mL beaker containing 100 mL of distilled water was placed beneath a glass funnel mounted on a ring stand. A test tube was positioned at the opening of the funnel to temporarily block the flow of the sample. 1 g of protein isolate was then added to the funnel. To begin the test, the test tube was removed, allowing the protein powder to flow freely into the beaker. The wettability was recorded as the time required for the entire powder sample to be fully wetted, with no floating dry particles visible.

2.3.3. Water binding capacity. 1 g of protein isolate sample was added to 10 mL of distilled water and agitated for 5 minutes. The solutions were left to stand for 30 minutes before being centrifuged at 4500 rpm for 30 minutes. After centrifugation, the supernatant was carefully removed, and the tubes were inverted at a 45° angle for 25 minutes to eliminate any residual liquid. Then the water binding capacity of untreated and CPT-modified RBPI was calculated using eqn (1):

$$\mathrm{WBC} = \frac{a-b}{c} \quad (1)$$

where, a is the mass of the tube with the absorbed water and protein isolates in grams (g), b is the mass of the protein isolate and tube in grams (g), and c is the mass of the RBPI in grams (g).

2.3.4. Emulsifying activity and emulsifying stability. A 5 mL aliquot of 2% (w/v) protein solution was homogenised with 5 mL of sunflower oil to form an emulsion. The homogenization process was carried out using a high-speed homogeniser (*e.g.*, IKA T25) at a speed of 10 000 rpm for 2 minutes, ensuring the thorough dispersion of the protein solution in the oil phase. The 5 mL volume of oil was chosen to simulate typical food emulsions, providing sufficient oil to allow for the formation of a stable emulsion and for subsequent measurement of emulsifying activity. Following homogenization, the prepared

emulsion was centrifuged at 3500 rpm for 5 minutes to separate the emulsified and non-emulsified phases. The total height of the content and the height of the emulsified layer in the tube were measured. The emulsifying activity of untreated and CPT-modified RBPI was calculated using eqn (2):

$$\text{Emulsifying activity (\%)} = \frac{\text{Height of emulsified layer}}{\text{Height of total content in the tube}} \times 100 \quad (2)$$

The same 5 mL aliquot of 2% (w/v) protein solution was homogenised with 5 mL of sunflower oil, using the same homogenization conditions as described for emulsifying capacity. The prepared emulsion was heated in a water bath at 80 °C for 30 minutes to simulate typical food processing conditions. After heating, the emulsion was centrifuged at 3500 rpm for 5 minutes to separate the phases.[34] The height of total content and that of the emulsified layer in the tube were noted, and the emulsifying stability of untreated and CPT modified RBPI was calculated using eqn (3):

$$\text{Emulsifying stability (\%)} = \frac{\text{Height of emulsified layer}}{\text{Height of total content in the tube}} \times 100 \quad (3)$$

2.3.5. Foaming capacity and foaming stability. The 3 g of protein isolate were mixed with 100 mL of distilled water, and the solution was whipped at high-speed using a mixer blender for five minutes. The resulting foam was then transferred into a measuring cylinder, and its initial volume was recorded. Changes in foam volume were subsequently measured at 15, 30, 45, and 60 minutes.[35] The foaming capacity and foaming stability untreated and CPT-modified RBPI were calculated using eqn (4) and (5), respectively:

$$\text{Foaming capacity (\%)} = \frac{\text{Volume after whipping} - \text{volume before whipping}}{\text{Volume before whipping}} \times 100 \quad (4)$$

$$\text{Foaming stability (\%)} = \frac{\text{Foam volume after time } (t)}{\text{Initial volume}} \times 100 \quad (5)$$

2.4. Change in carbonyl content

The dispersions of untreated and CPT-modified RBPI were made in distilled water having a concentration of 5 mg mL^{-1}. The dispersions were mixed in a magnetic stirrer for 30 minutes at room temperature. Then, in 1 mL of protein dispersion, 3 mL of DNPH (10 mM made in 2 M (HCl)) was added and incubated for 2.5 hours at room temperature. Then, 4 mL of 20% trichloroacetic acid (TCA-20%) was added to the solution, and it was rested for 10 minutes. To collect the protein precipitate, the solution was centrifuged at 7000 rpm for 30 minutes. The pellets were washed and centrifuged with 5 mL of ethyl acetate/ethanol mixture (1 : 1, v/v) at 7000 rpm for 30 minutes to remove the free DNPH. The respective sample blanks were prepared in a mixture containing 3 mL of 2 M HCl (without adding DNPH) and 4 mL of TCA. Subsequently, the added precipitate in 3 mL of 6 M guanidine HCl (0.1 M sodium phosphate, pH 2.3) was kept for 20 minutes to ensure protein dissolution. Then the aliquots were centrifuged at 10 000 rpm for 5 minutes to remove the undissolved particles in the solution. The supernatants were measured for absorbance at 375 nm in a Labman LMSPUV1000B-ultraviolet-visible double beam spectrophotometer. The carbonyl group content of RBPI was calculated from absorbance (nm) values using the Beer–Lambert law (eqn (6)).

$$A = \varepsilon L c \quad (6)$$

where, A is the absorbance value, ε is the molar extinction coefficient of hydrazones (22 000 M^{-1} cm^{-1}), L is the path length (1 cm), and c is the carbonyl content (nmol mg^{-1}).

2.5. UV-visible spectroscopy

Untreated and CPT-modified RBPI were diluted to 0.025 mg mL^{-1} in deionized water, where untreated RBPI was used as a blank control, and the samples were scanned by Labman LMSPUV1000B ultraviolet-visible (UV-vis) double-beam spectrophotometer (Labman Scientific Instruments Pvt. Ltd, India). In the spectral range of 180–300 nm and was calibrated prior to analysis using standard reference materials.

2.6. Fourier transform infrared spectroscopy

FTIR spectroscopy of untreated and cold plasma-treated RBPI was performed using an Alpha-E FTIR spectrometer (Bruker Optics, Germany). Prior to analysis, each sample was finely ground and dried in a desiccator to minimize moisture interference. Approximately 1–2 mg of dried RBPI was mixed with ~100 mg of spectroscopic-grade KBr using a mortar and pestle to obtain a homogeneous powder, and the pellets were prepared for each sample. The spectra were recorded at a resolution of 4 cm^{-1} over the range 4000–500 cm^{-1} at room temperature. A total of 64 scans were co-added for each measurement to enhance the signal-to-noise ratio, allowing reliable detection of subtle differences in protein secondary structure.

2.7. Crystallography

X-ray diffraction (XRD) patterns of untreated and cold plasma-treated RBPI samples were recorded using a D8 Advance A25 diffractometer (Bruker, Germany). Diffractograms were collected over a 2θ range of 10–50°, with a scan rate of 1.20° min^{-1}.

2.8. Surface morphology

SEM was used to analyse the structural alterations in both untreated and cold plasma-treated RBPI samples using a field-emission scanning electron microscope (FESEM, Nova Nano-SEM; FEI, USA). Protein samples were mounted on aluminium stubs using double-sided conductive carbon tape, followed by platinum sputter-coating to obtain an electrically conductive surface. Imaging was performed at an accelerating voltage of 20 kV. Micrographs for all samples were captured at

magnifications ranging from 4000× to 5000×, depending on the structural features being observed.

2.9. Particle size distribution

The particle distribution of untreated and cold plasma-treated RBPI was measured using a Mastersizer 3000 (Malvern, model v3.70), as described by Both *et al.*[36] A total of 2 g of protein isolate in powder form was loaded into the dry dispersion unit, and analysis was conducted at 25 °C to maintain consistency.

2.10. SDS-PAGE analysis

The SDS-PAGE of untreated and CPT-modified RBPI samples was performed according to the method described by Kheto *et al.*[37] with minor modifications. The sample (5 mg mL^{-1}) was initially mixed with 6× loading dye (5 : 1) and boiled for 10 minutes at 95 °C. Then, 10 μL of the prepared solution was loaded in the gel lane, which comprised 4% stacking gel and 15% resolving gel. Initially, the electrophoresis voltage of the concentrated gel was 80 V, and then was adjusted to 120 V when the bands ran into the separating gel. The gel was then stained with Coomassie Brilliant Blue R-250 (0.05%) for 30 minutes and then destained until the background became transparent.

2.11. Rheology

The effect of temperature on the rheological properties of untreated and cold plasma-treated RBPI was analysed using dynamic oscillatory rheological measurements.[38] About 5 mL of protein dispersion (30% w/v) was loaded onto the lower plate, and the upper plate was lowered to contact the sample. The samples were subjected to a controlled temperature ramp from 20 °C to 110 °C at a constant heating rate of 2 °C min^{-1}. Oscillatory measurements were performed at a fixed frequency of 1 Hz and a strain amplitude of 0.5%, conditions previously determined to lie within the linear viscoelastic region (LVR) of the samples. Storage modulus (G'), loss modulus (G''), and loss tangent (δ) were monitored and measured throughout the process and measured.

2.12. Statistical analysis

All experiments were conducted in triplicate, and the results are expressed as mean ± standard deviation (SD). Statistical differences among treatments were evaluated using analysis of variance (ANOVA), followed by Duncan's multiple range test (DMRT) to determine significant differences at $p < 0.01$.

3. Results and discussion

3.1. Functional properties of rice bean protein isolate

Functional properties for sample A (untreated) and cold plasma treated samples B (10 kV for 5 minutes), C (10 kV for 10 minutes), D (10 kV for 20 minutes), E (20 kV for 5 minutes), F (20 kV for 10 minutes) and G (20 kV for 20 minutes) were analysed and compared. The properties measured were solubility, wettability, water binding capacity, emulsifying activity, emulsifying stability, foaming capacity and stability.

3.1.1. Solubility. There was a significant ($p < 0.01$) improvement in the solubility of RBPI after CPT. The solubility of sample A (untreated) was 71.95 ± 0.04%, whereas CPT-treated samples exhibited values of 82.39 ± 0.04% (B), 82.68 ± 0.05% (C), 89.21 ± 0.05% (D), 73.49 ± 0.04% (E), 88.14 ± 0.05% (F), and 72.23 ± 0.04% (G), as shown in Table 1. Overall, CPT enhanced protein solubility compared with the untreated sample; however, the effect varied depending on voltage and exposure duration. Sample D (10 kV, 20 minutes) yields the highest value (89.21 ± 0.05%). The increase in solubility can be attributed to structural unfolding and exposure of hydrophilic regions, which promote protein–water interactions. At higher plasma voltage (20 kV), sample F (10 minutes) retained a high solubility (88.14 ± 0.05%), suggesting an optimal balance between molecular unfolding and oxidative modification. In contrast, samples E (5 minutes) and G (20 minutes) with lower solubility (73.49 ± 0.04% and 72.23 ± 0.04%, respectively), indicating that excessive plasma exposure or very short exposure may lead to structural rearrangement, aggregation, or oxidative cross-linking, reducing the number of hydrophilic sites available for water binding. This pattern reflects a non-linear response, where moderate plasma energy enhances solubility, but overexposure results in partial denaturation and reduced hydration capacity.[39] The CPT reduces protein particle size, as confirmed by SEM and particle size analysis, facilitating greater protein–water interactions. Additionally, a higher negative charge reduces intermolecular aggregation, increasing the availability of interaction sites for water molecules and

Table 1 Functional properties of untreated and cold plasma treated rice bean protein isolate (RBPI)[a]

	Solubility (%)	Wettability (in seconds)	Water binding capacity (g g^{-1})	Foaming capacity (%)	Foaming stability (%)	Emulsifying activity (%)	Emulsifying stability (%)
A	71.95 ± 0.046^{a}	18.52 ± 1^{b}	2.09 ± 0.08^{a}	33.3 ± 1.34^{a}	93.7 ± 1.8^{f}	30 ± 2.15^{b}	$25 \pm 1.35^{a,b}$
B	82.39 ± 0.048^{d}	30.8 ± 0.6^{d}	2.73 ± 0.14^{a}	100 ± 1.58^{b}	0 ± 0.7^{a}	12 ± 1.57^{a}	12.5 ± 1.73^{a}
C	82.68 ± 0.059^{e}	$18.7 \pm 0.8^{b,c}$	2.51 ± 0.19^{a}	113.3 ± 1.47^{c}	$11.7 \pm 1.5^{b,c}$	28 ± 1.86^{b}	41.6 ± 0.8^{d}
D	89.21 ± 0.058^{g}	$19.2 \pm 0.5^{b,c}$	$3.97 \pm 0.04^{b,c}$	120 ± 0.95^{d}	22.2 ± 1.65^{e}	64 ± 1.78^{e}	38.8 ± 1.4^{d}
E	73.49 ± 0.044^{c}	20 ± 0.2^{c}	1.94 ± 0.04^{a}	140 ± 1.78^{e}	$14.3 \pm 1.54^{c,d}$	50 ± 2.67^{c}	$25 \pm 1.59^{b,c}$
F	88.14 ± 0.050^{f}	16 ± 0.8^{a}	1.45 ± 0.11^{a}	300 ± 1.31^{g}	11.1 ± 1.45^{b}	58 ± 1.87^{d}	28.1 ± 1.64^{c}
G	72.23 ± 0.049^{b}	15 ± 0.9^{a}	4.93 ± 0.06^{b}	166.6 ± 1.56^{f}	16 ± 2.51^{d}	57 ± 1.32^{d}	52.1 ± 0.97^{e}

[a] A – untreated, B – CPT 10 kV for 5 minutes, C – 10 kV for 10 minutes, D – 10 kV for 20 minutes, E – 20 kV for 5 minutes, F – 20 kV for 10 minutes, G – 20 kV for 20 minutes. The superscripts (a–g) indicate the significant effect ($p < 0.001$) of cold plasma treatment on rice bean protein isolate.

enhancing protein solubility.[40] CPT also introduces polar groups with oxygen at the plasma–protein interface, which further enhances solubility.[41]

Although solubility increased after CPT, samples treated at E (20 kV for 5 minutes) and G (20 kV for 20 minutes) exhibited lower solubility than those treated at 10 kV. This was due to prolonged treatment leading to excessive interactions with hydrophobic groups and the formation of large, insoluble complexes that promote aggregation. A similar pattern was noted by Wang *et al.*[42] and Zhang *et al.*,[43] where solubility initially increased after CPT but declined with prolonged exposure.[42,43] The highest solubility (89.20 ± 0.05%) was observed for sample D (10 kV for 20 minutes).

3.1.2. Wettability. Protein wettability is influenced by protein particle size and microstructure, surface polarity, topography, roughness, and surface area. Reducing wettability time is essential for optimising hydrophobic material properties and enhancing stability at the protein interface.[44] As shown in Table 1, the wettability time for sample A (untreated) was 18.52 ± 1 s. After CPT, wettability time increased for samples B, D, and E to 30.8 ± 0.6, 19.2 ± 0.5, and 20 ± 0.2 s, respectively, while samples C and F showed no significant ($p < 0.01$) change, likely due to minimal alterations in the hydrophilic ends of the protein. However, sample G exhibited a significant reduction in wettability time (15 ± 0.9 s), possibly due to a decrease in surface tension and an increase in protein solubility.[45] Dong *et al.*[46] reported that the surface wettability of zein protein improved after CPT, which was attributed to increased surface roughness from bombardment or etching and the enrichment of polar functional groups.[46] Similarly, An *et al.*[47] stated that powders with 60 seconds or less wettability time are considered easy to wet, while those exceeding 120 seconds are classified as non-wettable. Based on these criteria, all untreated and cold plasma-treated samples demonstrated good wettability properties.

3.1.3. Water binding capacity. The water binding capacity of sample A (untreated) was 2.09 ± 0.08. CPT significantly enhanced the water-binding capacity of modified proteins. As shown in Table 1, sample G (treated at 20 kV for 20 minutes) exhibited a twofold increase, reaching 4.93 ± 0.06. Additionally, improvements were observed in samples B (2.73 ± 0.14), C (2.51 ± 0.08), and D (3.97 ± 0.04), demonstrating the positive effect of CPT on protein hydration properties. However, samples E (1.94 ± 0.04) and F (1.45 ± 0.11) exhibited a lower water binding capacity. This reduction at higher plasma intensities can be attributed to excessive oxidation and structural cross-linking of protein molecules, which decreases the availability of hydrophilic sites and restricts water penetration. Such overexposure can lead to the formation of compact, rigid networks with fewer accessible polar groups, thereby limiting water-binding ability despite initial unfolding. It is important to note that water-binding capacity values are expressed per gram of the initial protein isolate. Because cold plasma treatment affects protein solubility, the amount of material recovered after centrifugation may differ among samples. Thus, the measured water binding capacity reflects the hydration behaviour of the overall protein system, not only the insoluble residue. Consequently, variations in water binding capacity across samples A–G represent the combined effects of plasma-induced unfolding, aggregation, oxidation, and changes in solubility. According to Abarghoei *et al.*,[48] the water-holding capacity of samples increased with an increase in time of CPT because of the attachment of ROS groups with the surface of the protein, which strongly interacts with water and holds it efficiently.[48] When highly exposed, ionizable polar amino acids can also alter protein water-holding capacity. The water-binding capacity of the protein increases with CPT due to increased hydrophilicity.[49] According to Mehr and Koocheki,[50] higher water binding capacity is associated with higher degradation of primary protein aggregates and oxidation of amino acid residues into polar groups (carboxyl and carbonyl groups).[51] The difference in water binding capacity can also be attributed to the exposure of charged and polar sites in the polypeptide chain, the hydrophobic nature, and the flexible structure.[37] Tan *et al.*[52] also observed that cold plasma may increase WBC through oxidative cross-linking and carbonyl group formation, but beyond the optimum energy threshold, over-oxidation reduces hydrogen bonding sites. Therefore, the observed decrease in WBC in samples E and F reflects the non-linear response of proteins to plasma treatment, where moderate exposure enhances hydration, while excessive oxidation at higher voltages and longer durations diminishes water-binding ability.

3.1.4. Emulsifying properties. As shown in Table 1, the emulsifying activity for sample A (untreated) was 30 ± 2.15%. After CPT, sample D showed a 2-fold increase in emulsifying activity, *i.e.*, 64 ± 1.78%, followed by samples F (58 ± 1.87%), G (57 ± 1.32%), and E (50% ± 2.67). On the other hand, the emulsifying activity of samples B and C was reduced to 12 ± 1.57% and 28 ± 1.68%, respectively. The emulsifying stability for untreated protein was 25 ± 1.35%. After CPT, sample G showed a 2-fold increase in emulsifying stability, *i.e.*, 52.1 ± 0.97%, followed by samples C (41.6 ± 0.8%), D (38.8 ± 1.4%), and F (28.1 ± 1.64%). Whereas the emulsifying stability of sample B was observed to be reduced to 12.5 ± 1.73%. However, no significant effect is observed for the emulsifying stability of samples E and A.

Due to CPT, the protein structure loosens and optimises protein distribution at the oil–water interface, improving emulsifying activity. Additionally, plasma treatment causes protein oxidation, thereby, enhancing the dispersion of protein aggregates and, in turn, enhancing its functionality.[53] According to Mehr and Koocheki,[50] when protein was treated for 5 minutes in cold plasma, there was an interaction of the ROS group with the protein surface, therefore, creating a hydrophobic/hydrophilic balance and increasing emulsifying capacity.[54] However, excessive oxidation can lead to the aggregation of protein aggregates, decreasing their functionality, as observed in samples B and C.[44] It can also be due to the fragmentation of protein molecules, leading to decreased activation of interfacial tension. CPT results in the unfolding of the protein, thereby changing its secondary structure, increasing the β-sheet content, resulting in reduced and reducing interfacial tension within the protein. Consequently, it rapidly absorbs into the oil–water interface.[49]

3.1.5. Foaming properties. As peptides unfold, a protective layer is formed at the interface, facilitating foam formation. As depicted in Table 1, the foaming capacity of sample A (untreated) was recorded at 33 ± 1.34%. The foaming capacity for CPT-RBPI samples was observed to be increased with increase in voltage and time and observed to be highest in sample F (300 ± 1.31%), followed by samples G (166.6 ± 1.56%), E (140 ± 1.78%), D (120 ± 0.95%), C (113.3 ± 1.47%) and B (100 ± 1.58%). After CPT, sample F exhibited a ninefold increase in the foaming capacity. The increase in foaming capacity was attributed to enhanced protein solubility.[54]

CPT enhances protein solubility, allowing modified protein molecules to rapidly absorb at the air–water interface due to increased electrical charge. This charge enhancement improves protein–water interactions, promoting faster molecular movement to the interface and reducing surface tension.[43] The unfolding of proteins due to CPT makes the structure more flexible and allows it to arrange itself at the air–water interface.[49] The increase in foaming capacity with higher applied voltage is due to the higher energy of the plasma etching process, leading to accelerated dissociation of protein and a decrease in intermolecular aggregate, leading to enhanced conformational flexibility and exposure of hydrophobic ends. Therefore, more protein molecules are accessible for foaming.[54] Foams are complex systems that are thermodynamically unstable and always reorganise to create lower-energy structures.[55] The stability of the foam for sample A remained at 100% for 45 minutes; however, it decreased to 93.7 ± 1.8% at the 60th minute, as depicted in Table 1. However, after CPT, the foaming stability gradually decreased, and in the 15th minute, the foaming stability for samples B, C, D, E, F, and G was 13.3 ± 1.7%, 29.4 ± 1.4%, 22.2 ± 1.46%, 19 ± 1.82%, 11.1 ± 1.27% and 48 ± 2.14% respectively. It is due to the development of a weak surface layer surrounding the air bubbles, which is linked to the loss of protein conformational stability, low secondary structural rigidity, and distortion of intra- and intermolecular contacts. Therefore, CPT improves the hydrophobic/hydrophilic balance and enhances the functional properties of rice bean isolate protein, including wettability, water binding capacity, emulsifying capacity, and foaming capacity. However, the foaming stability of the cold plasma-treated samples was lower than that of the untreated protein.

3.2. Changes in carbonyl groups

The carbonyl content of RBPI subjected to CPT is presented in Fig. 2. The untreated sample exhibited a baseline carbonyl content of 5.33 nmol mg^{-1} protein. Upon plasma treatment at 10 kV for 5 minutes, the carbonyl content increased to 6.54 nmol mg^{-1}, indicating initial oxidative modification. Further extension of treatment time at 10 kV resulted in a significant increase in carbonyl levels, reaching 10.97 nmol mg^{-1} at 10 minutes and 15.66 nmol mg^{-1} at 20 minutes. At a higher voltage of 20 kV, a pronounced increase in carbonyl content was observed. Treatment for 5 minutes yielded 17.55 nmol mg^{-1}, which further escalated to 20.70 nmol mg^{-1} at 10 minutes and 20.96 nmol mg^{-1} at 20 minutes. Notably, the carbonyl content appeared to plateau beyond 10 minutes at 20 kV, suggesting a saturation effect.

The increase in carbonyl content following CPT reflects oxidative modification of RBPI. Cold plasma generates reactive

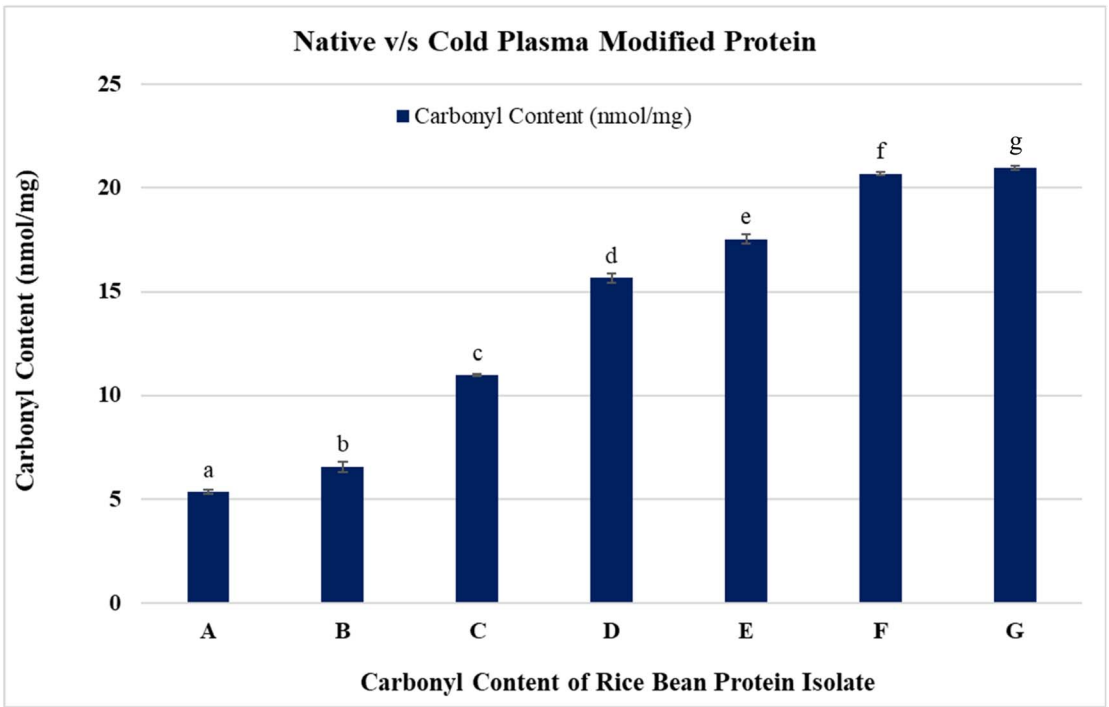

Fig. 2 Carbonyl content of untreated and cold plasma-treated rice bean protein isolate. Treatments: A – untreated; B – CPT 10 kV, 5 minutes; C – 10 kV, 10 minutes; D – 10 kV, 20 minutes; E – 20 kV, 5 minutes; F – 20 kV, 10 minutes; G – 20 kV, 20 minutes. Different superscripts (a–g) indicate significant differences ($p < 0.001$) among treatments.

oxygen and nitrogen species (ROS and RNS), which interact with susceptible amino acid residues (lysine, arginine, proline, and threonine), leading to carbonyl formation. The results demonstrated that both voltage intensity and treatment duration have a significant impact on the extent of oxidation. The dose-dependent rise in carbonyl levels from 10 kV to 20 kV and from 5 to 20 minutes of treatment suggests progressive protein modification. These findings are consistent with earlier reports on soy protein and pea protein isolates, where increased plasma exposure elevated protein oxidation markers.[56,57] Importantly, the plateau observed at 20 kV beyond 10 minutes indicates a potential saturation point, where most reactive sites on the protein are oxidized, and further treatment does not significantly increase carbonyl formation. This suggests that plasma treatment parameters need to be optimized to achieve maximum modification without incurring unnecessary energy input. Protein oxidation through carbonylation can influence the functional properties of RBPI.

3.3. UV absorption analysis

Fig. 3 depicts the ultraviolet spectra (A) and ultraviolet second-order reciprocal spectra (B) of RBPI modified CPT at different levels. The untreated sample (sample A) showed a baseline absorbance of 0.195. Upon exposure to cold plasma at 10 kV for 5 minutes (sample B), the absorbance increased to 0.227, indicating the onset of oxidative modification. A further increase in treatment time at 10 kV led to a progressive rise in absorbance, reaching 0.318 and 0.454 for 10 minutes (sample C) and 20 minutes (sample D), respectively. Treatment at a higher voltage of 20 kV resulted in a more substantial increase, with absorbance values of 0.678, 0.717, and 0.722 for treatment durations of 5, 10, and 20 minutes (samples E, F, and G, respectively). Notably, absorbance appeared to plateau beyond 10 minutes at 20 kV, suggesting that further treatment yielded minimal additional oxidation. The observed increase in absorbance correlates with the generation of oxidised protein products, particularly carbonyl derivatives that absorb in the UV-visible range.

This trend confirms that CPT induces oxidative modifications in RBPI, leading to the formation of chromophoric groups. These findings are consistent with previous studies where plasma treatment enhanced protein absorbance due to the accumulation of oxidised moieties.[20] The ultraviolet second-order reciprocal spectra of rice bean protein subjected to CPT exhibited progressive structural modifications corresponding to treatment intensity and duration. The untreated sample (A) displayed typical spectral characteristics of a native protein structure. Upon plasma exposure at 10 kV for 5 minutes (B) and 10 minutes (C), minor shifts in the second derivative around 260 nm suggested the onset of partial unfolding and initial exposure of peptide bonds. With prolonged treatment at 10 kV for 20 minutes (D), more pronounced changes emerged, including enhanced positive second derivative signals, indicative of greater structural loosening. At higher plasma intensities (20 kV), the structural modifications became more pronounced. Samples treated at 20 kV for 5 minutes (E) already showed noticeable perturbations in secondary structures, while longer exposures at 10 minutes (F) and 20 minutes (G) induced substantial alterations. Specifically, strong negative second derivative values beyond 280 nm in these samples implied oxidation or reorientation of aromatic amino acid residues such as tyrosine and tryptophan. The decrease in reciprocal absorbance between 220–240 nm across higher voltage and longer duration treatments also pointed to a disruption of α-helix and β-sheet formations. Collectively, the results suggest that CPT induces voltage- and time-dependent structural rearrangements in rice bean protein, transitioning from minor conformational shifts at lower intensities to extensive unfolding and oxidative modifications at higher intensities.

3.4. Fourier-transform infrared (FTIR) spectroscopy

In FTIR spectroscopy, the 1600–1700 cm^{-1} region corresponds to the amide I band, which primarily arises from the C=O stretching vibration of peptide bonds.[31,58,59] Absorption peaks within this range are indicative of the secondary structural

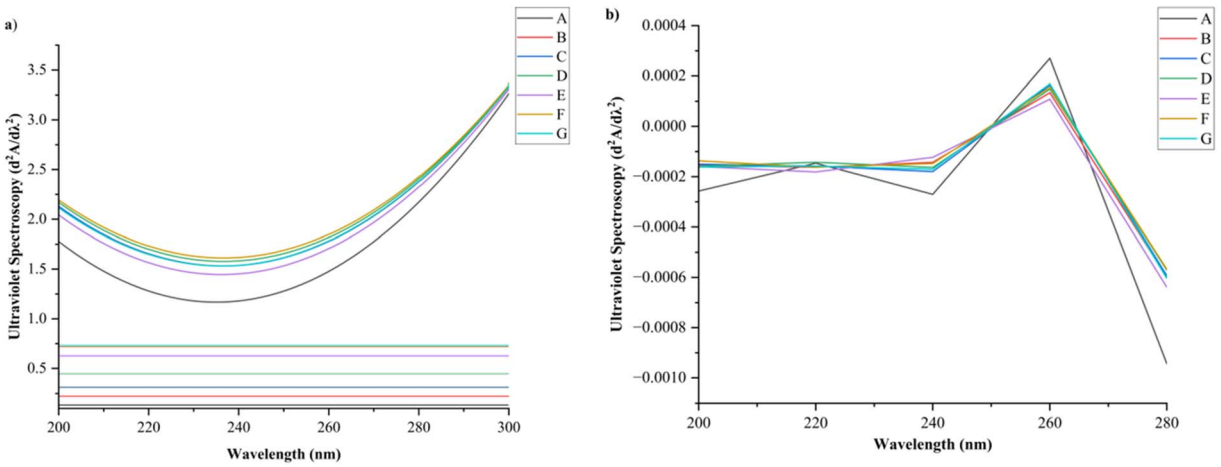

Fig. 3 Ultraviolet spectra (a) and ultraviolet second-order reciprocal spectra (b) of rice bean protein isolate treated by cold plasma. Treatments: A – untreated; B – CPT 10 kV, 5 minutes; C – 10 kV, 10 minutes; D – 10 kV, 20 minutes; E – 20 kV, 5 minutes; F – 20 kV, 10 minutes; G – 20 kV, 20 minutes.

conformations of proteins such as α-helices, β-sheets, turns, and random coils. According to Candoğan *et al.*,[59] the 1610–1620 cm^{-1} region corresponds to aggregated β-sheets, 1621–1640 cm^{-1} to β-sheets, 1641–1647 cm^{-1} to random coil/unordered structures, 1648–1657 cm^{-1} to α-helices, and 1660–1696 cm^{-1} to turns and bends (β-turns). As depicted in Fig. 4, the FTIR spectrum of sample A (untreated) exhibited a distinct absorption peak at 1692.8 cm^{-1}, which is assigned to the amide I (C═O stretching) vibration associated with β-turns and bends, in accordance with the range reported by Candoğan *et al.*[59] This indicates the presence of folded regions within the polypeptide chain stabilized by intramolecular hydrogen bonding. After CPT, the amide I peak shifted to 1714.4, 1694.9, 1706.7, 1691.7, 1675.6, and 1677.7 cm^{-1} for samples B, C, D, E, F, and G, respectively. These spectral shifts reflect modifications in the C═O stretching vibration of peptide bonds, suggesting conformational rearrangements in the protein secondary structure induced by plasma exposure. In sample C, the absorption peak at 1694.9 cm^{-1} corresponds to β-turns, which are formed due to folding of the peptide chain. In sample E, the band observed at 1675.6 cm^{-1} lies within the turns and bends region, suggesting increased flexibility and partial unfolding of the protein. Conversely, sample G exhibited a prominent peak near 1640 cm^{-1}, which is characteristic of β-sheet structures, indicating the reorganization of peptide chains into more ordered β-sheet arrangements.[60–62] Overall, these results demonstrate that CPT alters the protein's secondary structure by inducing transitions among β-turns, α-helix, and β-sheet conformations. The observed peak shifts in the amide I region confirm structural reorientation and modification of hydrogen bonding interactions within the rice bean protein isolate.

3.4.1. Crystallography. From Fig. 5, the major peaks at 2θ = 8°, 14°, 20°, 32.4°, and 40° were observed for sample A-untreated and CPT-RBPI, and samples B, C, D, E, F, and G. The samples exhibited two dominant amorphous haloes, broad bands with a maximum at 2θ = 14° and 20°. Pure protein isolates with 7S and 11S amorphous globulins as their primary constituents have a broad band with a maximum at $2\theta = 20°$.[63] After CPT, the intensity of the band at 20° increased in sample B, depicting a higher order of the structure.[64]

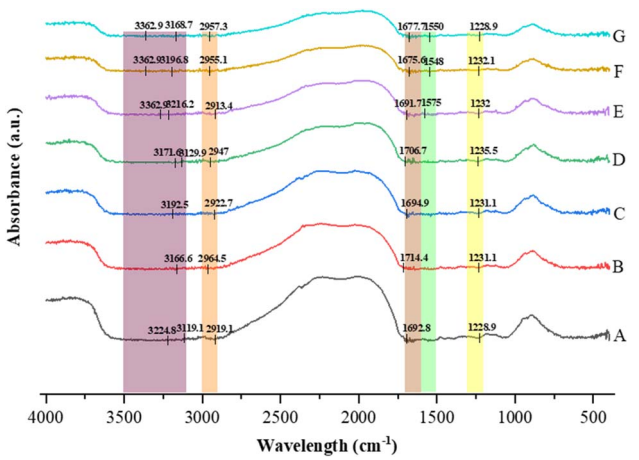

Fig. 4 FTIR spectroscopy of untreated and cold plasma-treated rice bean protein isolate. Treatments: A – untreated; B – CPT 10 kV, 5 minutes; C – 10 kV, 10 minutes; D – 10 kV, 20 minutes; E – 20 kV, 5 minutes; F – 20 kV, 10 minutes; G – 20 kV, 20 minutes.

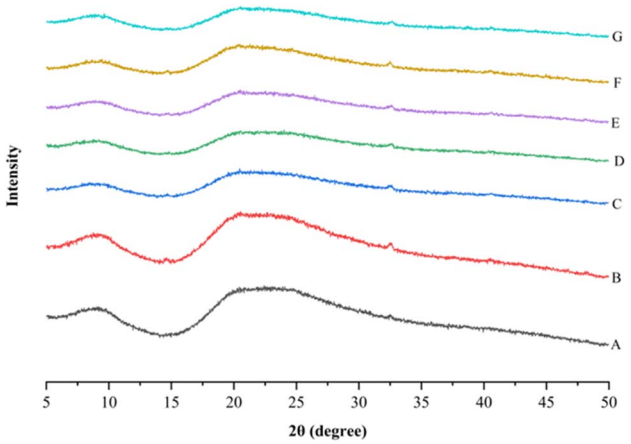

Fig. 5 X-ray diffraction characterization for untreated and cold plasma-treated rice bean protein isolate: treatments: A – untreated; B – CPT 10 kV, 5 minutes; C – 10 kV, 10 minutes; D – 10 kV, 20 minutes; E – 20 kV, 5 minutes; F – 20 kV, 10 minutes; G – 20 kV, 20 minutes.

The samples showed a peak in crystalline region II, *i.e.*, 2θ = 20°, with a broad band indicating the amorphous nature of the rice bean protein isolates.[64] The XRD pattern peak at 20° is a characteristic feature of the β-sheet structure.[65] Therefore, the diffraction peaks observed at 2θ = 20° for all untreated and treated protein samples showed the dominance of β-sheets of their secondary structures. In the XRD pattern, the intensity of the peak at 2θ = 20° increased after CPT, inferring an increase in the percentage of β-sheet in the protein isolate.[66] XRD pattern showing a broad peak within the 13°–23° range indicates the amorphous nature of all the samples.

3.5. Surface morphology

SEM was used to analyse the morphology of proteins, comprehending the impact of processing on the surface. The surface of sample A (untreated) appeared to be irregular, spherical, rough, and aggregated, as depicted by Fig. 6. This bulky and dense structure is due to the cross-linking of peptide bonds.[45] Protein samples became coarser and more loosely bonded as the treatment time increased, compared to the surface of the untreated sample. As plasma treatment increased from sample B to E, the aggregates began to disperse, expanding RBPI molecules and increasing exposure of hydrophobic groups, suggesting enhanced unfolding and aggregation driven by plasma-induced modifications.[22] The 5-minute treatment at 20 kV (Fig. 6E) exhibited a more open porous structure with large voids, indicative of protein denaturation and reorganisation. Longer treatments at 20 kV for 10 minutes (Fig. 6F) and 20 minutes (Fig. 6G) resulted in extensive network formation with an irregular, porous morphology and interconnected channels. This suggests that cold plasma at higher voltages and duration promoted extensive cross-linking and aggregation, leading to a more developed gel-like microstructure. According to Ge *et al.*,[19] it is due to the increased surface etching as the accumulation of reactive species

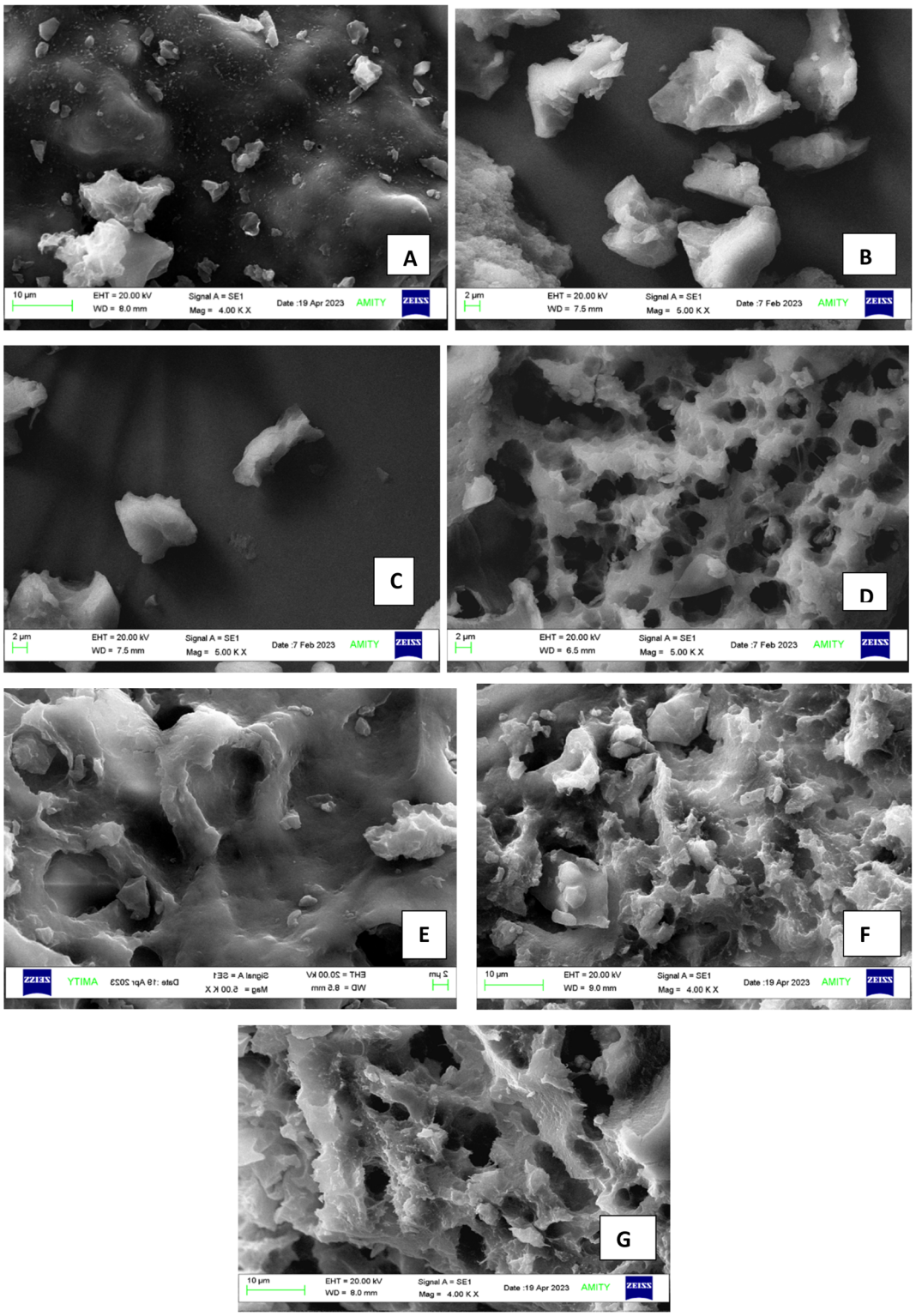

Fig. 6 SEM analysis for untreated and cold plasma-treated rice bean protein isolate: treatments: A – untreated; B – CPT 10 kV, 5 minutes; C – 10 kV, 10 minutes; D – 10 kV, 20 minutes; E – 20 kV, 5 minutes; F – 20 kV, 10 minutes; G – 20 kV, 20 minutes.

increases, leading to a reduction in the crystalline structure and reorientation of the structural orientation.[19,67]

Two types of reactions can cause plasma species to etch the surface of biopolymers: (i) a physical sputtering reaction resulting from inelastic collisions between the surface of the biopolymer and excited particles of the plasma, such as electrons, and (ii) a chemical reaction that generates volatile gaseous and radicals within the biopolymer matrix.[68,69] CPT causes an increase in the specific surface area, directly increasing the exposure of the active site. It becomes easier for

a reactive free radical environment to react more quickly, causing accelerated protein oxidation.[70] The surface of the protein uses optical radiation phenomena to absorb plasma energy discharge, leading to changes in surface morphology due to the ongoing influence of optical radiation energy.[71] Fig. 6 depicts the images of sample A (untreated) and CPT-RBPI at different treatment levels. The CPT modifies the secondary structure (mainly β-structures) of isolated powder and inhibits protein aggregation. The friction, collision, and shear forces caused by plasma alter the surface morphology of the RBPI aggregate, leading to changes in the structural network.

3.6. Particle size distribution

As shown in Table 2, sample A exhibited relatively large particle sizes with $D_x(50) = 190$ μm and a broad distribution ($D_x(90) = 394$ μm), indicating extensive aggregation within the native protein system. After CPT, a substantial reduction in the median particle size ($D_x(50)$) was observed in all treated samples, demonstrating disorder and enhanced dispersion. At 10 kV treatments (samples B–D), the $D_x(50)$ values decreased sharply from 190 μm to approximately 128–134 μm, reflecting the initial breakdown of aggregates. At a higher voltage (20 kV), the particle size further decreased, with sample F (20 kV, 10 minutes) showing the lowest median particle size ($D_x(50) = 127$ μm), representing maximum disintegration and stabilization of the protein particles. It can be due to the depolymerisation of protein macromolecules. Several free radicals were produced by the particle collisions, and these radicals had the potential to either introduce active sites or oxidize amino acids on the protein surface.[53] This process has the potential to cause protein disintegration by weakening the force between protein molecules, micelles, and destroying chemical links on the protein's surface. Furthermore, this reduction in particle size correlates well with the SEM observations, where treated samples showed increased porosity and fragmented structures.[20] However, in sample G (20 kV, 20 minutes), a slight increase in particle size ($D_x(50) = 128$ μm and $D_x(90) = 317$ μm) was observed. This marginal rise can be attributed to partial re-aggregation or re-association of protein molecules after prolonged plasma exposure. Extended treatment duration may lead to oxidative cross-linking and the formation of intermolecular bonds, promoting limited agglomeration and thereby increasing the apparent particle size. Such non-linear behavior has been reported in previous studies,[40,72] where extended plasma treatment caused secondary aggregation due to oxidation of amino acid side chains and alterations in surface hydrophobicity.

Table 2 Particle size parameters of untreated and cold plasma-treated RBPI

Sample/ treatment	Treatment description	$D_x(10)$ (μm)	$D_x(50)$ (μm)	$D_x(90)$ (μm)
A	Untreated	74.9	192	395
B	10 kV, 5 minutes	32.5	132	340
C	10 kV, 10 minutes	32.0	130	314
D	10 kV, 20 minutes	32.9	125	305
E	20 kV, 5 minutes	32.0	128	315
F	20 kV, 10 minutes	32.6	120	291
G	20 kV, 20 minutes	33.1	124	296

3.7. SDS-PAGE analysis

SDS-PAGE analysis (Fig. 7) revealed that the overall molecular weight distribution of RBPI remained largely unchanged after cold plasma treatment. The major protein bands (~55 kDa, ~40 kDa, and lower-molecular-weight fractions) were retained across all treatments (A–G), indicating that plasma exposure did not induce extensive peptide backbone cleavage detectable under denaturing electrophoretic conditions. However, subtle but meaningful alterations were observed in agreement with other structural indicators. At higher voltage and longer durations (20 kV; lanes E–G), a slight reduction in the sharpness and intensity of bands in the lower molecular weight region was noted, accompanied by mild smearing. These features are characteristic of side-chain oxidation, partial unfolding, and limited aggregation, processes that do not necessarily produce new discrete molecular weight fragments but are consistent with the significant increase in carbonyl content (Fig. 2). The pronounced reduction in particle size (Table 2) also supports these interpretations. Cold plasma-induced oxidation can weaken noncovalent interactions and modify surface functional groups, leading to the disintegration of supramolecular protein assemblies without major changes to the primary structure, which explains the decreased $D_x(50)$ values while maintaining similar SDS-PAGE band positions. The slight reaggregation observed in sample G in particle size analysis aligns with the faint smearing at stronger plasma conditions.

These results align with previous reports,[41,73] where moderate plasma treatment altered protein functional groups without causing major structural disruption. The preserved primary structure suggests that cold plasma can effectively tailor protein functionality while maintaining molecular integrity.

3.8. Rheological behaviour

The viscoelastic behaviour of untreated and cold plasma-treated RBPI was evaluated through temperature sweep tests, as presented in Fig. 8(a, b and c), showing storage modulus (G'), loss modulus (G''), and loss factor (tan δ), respectively.[74,75]

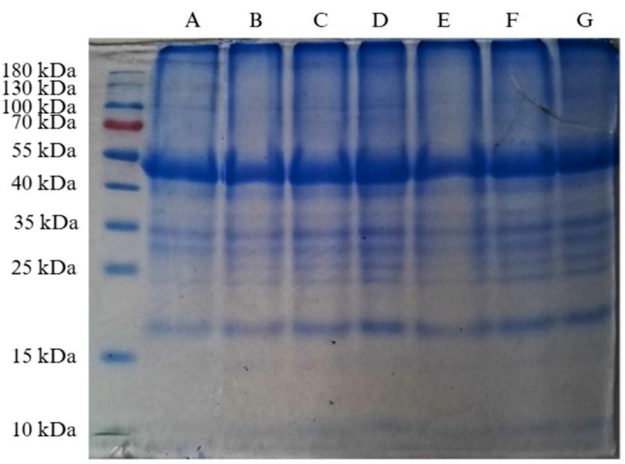

Fig. 7 SDS-PAGE analysis for untreated and cold plasma-treated rice bean protein isolate. Treatments: A – untreated; B – CPT 10 kV, 5 minutes; C – 10 kV, 10 minutes; D – 10 kV, 20 minutes; E – 20 kV, 5 minutes; F – 20 kV, 10 minutes; G – 20 kV, 20 minutes.

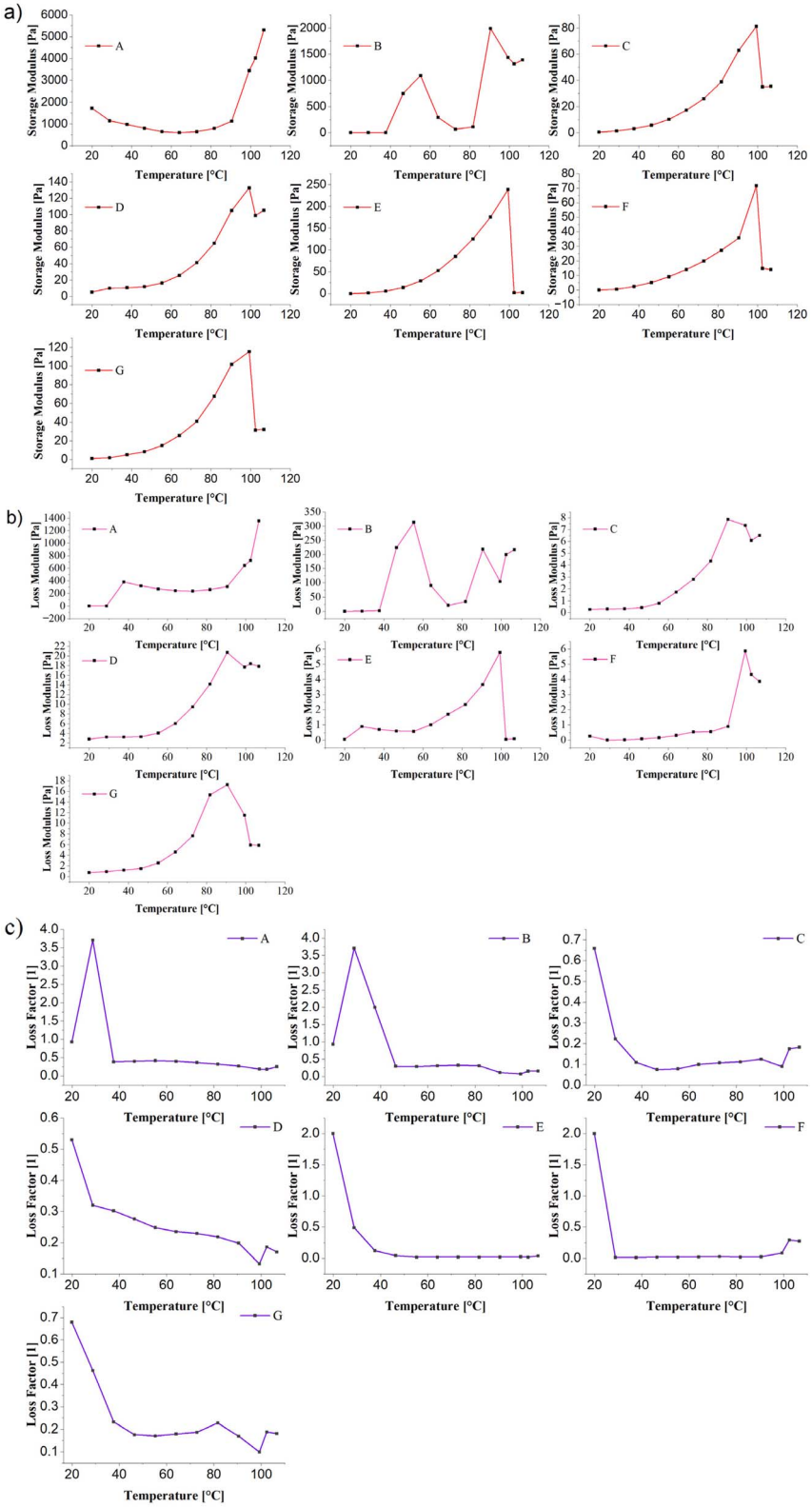

Fig. 8 Temperature sweep curves showing the storage modulus (G') (a); temperature sweep curves showing the loss modulus (G'') (b) and temperature sweep curves showing the loss factor ($\tan\delta$) (c) of untreated and cold plasma-treated rice bean protein isolate (RBPI). Treatments: A – untreated; B – CPT 10 kV, 5 minutes; C – 10 kV, 10 minutes; D – 10 kV, 20 minutes; E – 20 kV, 5 minutes; F – 20 kV, 10 minutes; G – 20 kV, 20 minutes.

3.8.1. Storage modulus (G'). The untreated RBPI (sample A) displayed a typical biphasic pattern in G' with increasing temperature. An initial decline was observed up to ~70 °C, indicating the disruption of weak intermolecular forces, followed by a sharp rise beyond 80 °C, corresponding to protein denaturation and network formation, which peaked near 105 °C. Plasma treatment significantly modified this behaviour. Sample B (10 kV, 5 minutes) exhibited fluctuating G' values with a prominent peak around 100 °C, suggesting enhanced thermal responsiveness due to partial unfolding.[76] Samples C (10 kV, 10 minutes) and D (10 kV, 20 minutes) showed steadily increasing G' up to 100 °C, indicating progressive protein–protein interactions and network structuring. At 20 kV, sample E (5 minutes) demonstrated the highest G' peak at 100 °C, suggesting optimal cross-linking. In contrast, longer treatments (samples F and G) showed lower G' peaks, implying that excessive plasma exposure causes structural over-modification or degradation, reducing gel strength.

3.8.2. Loss modulus (G''). The loss modulus (G''), which reflects the viscous nature and energy dissipation of the samples, followed similar but less pronounced trends.[77] Untreated RBPI (A) showed an increase in G'' beyond 80 °C, peaking near 105 °C, indicating increased molecular mobility during gelation. Plasma-treated samples exhibited treatment-dependent variations. Samples B and E exhibited multiple sharp peaks, indicating intermittent relaxation phenomena resulting from structural transitions induced by plasma treatment. Samples C, D, F, and G displayed gradual increases in G'' up to 100 °C, supporting the notion of enhanced viscous dissipation as protein structures reorganise. Notably, sample E (20 kV, 5 minutes) recorded a significant rise in G'', indicating a balanced viscoelastic response ideal for forming stable gels.

3.8.3. Loss factor ($\tan\delta$). The loss factor ($\tan\delta = G''/G'$) provides insight into the balance between elastic and viscous behaviour. For untreated RBPI, $\tan\delta$ initially spiked around 30 °C, then declined with increasing temperature, indicating a transition from a viscous-dominant to an elastic-dominant material upon heating and gelation. CPT markedly affected $\tan\delta$ values. Samples B, E, and F showed exceptionally high $\tan\delta$ at lower temperatures (20–30 °C), suggesting plasma-induced weakening of the elastic network and temporary dominance of viscous flow. However, at higher temperatures (>60 °C), $\tan\delta$ dropped sharply across all treated samples, confirming the establishment of an elastic gel network. Notably, samples C, D, and G maintained moderate $\tan\delta$ values throughout the heating cycle, indicating a more balanced viscoelastic character that is suitable for stable gel formation.

CPT at moderate conditions (particularly 20 kV for 5 minutes) enhanced both the storage and loss moduli, reflecting improved protein–protein interactions and gelation capacity. However, overexposure (longer times or higher voltage) resulted in reduced modulus values and excessive $\tan\delta$ at lower temperatures, indicating compromised structural integrity.[77] These findings suggest that plasma treatment fine-tunes the viscoelasticity of RBPI, where optimal treatment enhances elasticity and gel strength, whereas excessive modification leads to weakened networks.

4. Conclusion

The present study demonstrates that CPT effectively modulates the structural and functional properties of RBPI in a treatment-dependent manner. Spectroscopic analyses (FTIR and UV-vis) confirmed modifications in secondary structure and aromatic amino acid environments, indicating plasma-induced unfolding and rearrangement of protein conformations. SEM imaging further supported these observations by revealing significant alterations in surface morphology, while XRD analysis showed reduced. Crystallography analysis provided additional evidence of structural reorganisation, showing reduced crystallinity and increased amorphous character in plasma-treated proteins, which correlates with improved solubility and functional properties. UV spectroscopy revealed shifts in absorbance patterns and changes in second derivative spectra, indicating modifications in the microenvironment of aromatic residues and the overall protein conformation. Particle size analysis revealed a non-linear trend, with moderate plasma exposure reducing particle size and extended treatment promoting limited re-aggregation. SDS-PAGE confirmed that the primary structure remained intact, demonstrating that CPT selectively alters higher-order structures without degrading the protein backbone. Rheological evaluations revealed that moderate plasma treatment, especially at 20 kV for 5 minutes (sample E), enhanced both storage modulus (G') and loss modulus (G''), indicating improved protein–protein interactions and gelation capacity. Treated samples exhibited a favourable balance between elasticity and viscosity, forming stronger and more stable gel networks. In contrast, excessive treatment reduced modulus values and increased $\tan\delta$, indicating compromised network strength. These cumulative structural alterations translated into improved functional properties such as enhanced solubility, emulsifying activity, and foaming capacity at optimal treatment conditions, underscoring the potential of cold plasma as a non-thermal, clean-label technology to tailor protein functionality. Overall, the results confirm that cold plasma treatment is a promising strategy for improving the structural and functional attributes of rice bean protein isolate, broadening its application in food formulations.

Author contributions

Charu Agarwal: methodology, data curation, visualisation, formal analysis, writing – original draft. Rachna Sehrawat: formal analysis, writing – review and editing. Loveleen Sharma: conceptualisation, methodology, visualisation, formal analysis, supervision, writing – original draft, review and editing. Manoj Kumar Patel: methodology, visualisation, formal analysis, supervision, writing – review and editing.

Conflicts of interest

There are no conflicts to declare.

Abbreviations

CPT	Cold plasma treatment
RBPI	Rice bean protein isolate
WBC	Water binding capacity
ROS	Reactive oxygen species
RNS	Reactive nitrogen species
FTIR	Fourier infrared spectroscopy
XRD	X-ray diffraction
SEM	Scanning electron microscopy

Data availability

The data used are provided in the manuscript.

Acknowledgements

The authors would like to thank the Amity Institute of Food Technology, Amity University, Noida; Department of Food Process Engineering, National Institute of Technology, Rourkela, Odisha, and CSIR-Central Scientific Instruments Organisation, Chandigarh, for providing the resources to conduct this study.

References

1 K. Atta, S. Adhikary, S. Mondal, S. Mukherjee, A. Pal and S. Mondal, *et al.*, A review on stress physiology and breeding potential of an underutilized, multipurpose legume: Rice bean (Vigna umbellata), *Developing Climate Resilient Grain and Forage Legumes*, 2022, pp. 235–253.

2 R. Katoch, S. K. Sanadya, K. Pathania and H. Chaudhary, Nutritional and nutraceutical potential of rice bean (Vigna umbellata) – a legume with hidden potential, *Front. Nutr.*, 2023, **10**, 1126544.

3 A. Dahipahle, S. Kumar, N. Sharma, H. Singh, S. Kashyap and H. Meena, Rice bean – a multipurpose, underutilized, potential nutritive fodder legume: a review, *J. Pure Appl. Microbiol.*, 2017, **11**(1), 433–439.

4 B. R. Hoque, D. D. Wadikar and P. E. Patki, Rice bean: nutritional vibrant bean of Himalayan belt (Northeast India), *Nutr. Food Sci.*, 2016, **46**(3), 412–431.

5 R. Katoch, Nutritional potential of rice bean (Vigna umbellata): an underutilized legume, *J. Food Sci.*, 2013, **78**(1), C8–C16.

6 P. K. Dhillon and B. Tanwar, Rice bean: A healthy and cost-effective alternative for crop and food diversity, *Food Secur.*, 2018, **10**(3), 525–535.

7 A. Pattanayak, S. Roy, S. Sood, B. Iangrai, A. Banerjee, S. Gupta, *et al.*, Rice bean: a lesser-known pulse with well-recognized potential, *Planta*, 2019, **250**(3), 873–890.

8 D. R. Dash, S. K. Singh and P. Singha, Recent advances on the impact of novel non-thermal technologies on structure and functionality of plant proteins: a comprehensive review, *Crit. Rev. Food Sci. Nutr.*, 2024, **64**(10), 3151–3166.

9 O. O. Olatunde, I. O. Owolabi, O. S. Fadairo, A. Ghosal, O. J. Coker, O. P. Soladoye, *et al.*, Enzymatic modification of plant proteins for improved functional and bioactive properties, *Food Bioprocess Technol.*, 2023, **16**(6), 1216–1223.

10 F. U. Akharume, R. E. Aluko and A. A. Adedeji, Modification of plant proteins for improved functionality: a review, *Compr. Rev. Food Sci. Food Saf.*, 2021, **20**(1), 198–224.

11 H. B. Jadhav, U. S. Annapure and R. R. Deshmukh, Non-thermal technologies for food processing, *Front. Nutr.*, 2021, **8**, 657090.

12 S. Rout, R. K. Gupta, S. Sharma and P. P. Srivastav, Recent trends in the modification of plant proteins by non-thermal techniques: impact on functional properties and their application in food systems, *Eur. Food Res. Technol.*, 2025, 1–22.

13 M. Venkateswara Rao, S. CK, A. Rawson, C. DV and V. N, Modifying the plant proteins techno-functionalities by novel physical processing technologies: a review, *Crit. Rev. Food Sci. Nutr.*, 2023, **63**(19), 4070–4091.

14 F. A. Fernandes and S. Rodrigues, Cold plasma technology for sustainable food production: meeting the United Nations sustainable development goals, *Sustainable Food Technol.*, 2025, **3**(1), 32–53.

15 S. Chaple, C. Sarangapani, J. Jones, E. Carey, L. Causeret, A. Genson, *et al.*, Effect of atmospheric cold plasma on the functional properties of whole wheat grain and wheat flour, *Innovative Food Sci. Emerging Technol.*, 2020, **66**, 102529.

16 N. Sruthi, K. Josna, R. Pandiselvam, A. Kothakota, M. Gavahian and A. M. Khaneghah, Impacts of cold plasma treatment on physicochemical, functional, bioactive, textural, and sensory attributes of food: a comprehensive review, *Food Chem.*, 2022, **368**, 130809.

17 B. Kopuk, R. Gunes and I. Palabiyik, Cold plasma modification of food macromolecules and effects on related products, *Food Chem.*, 2022, **382**, 132356.

18 S. Zhang, W. Huang, M. Roopesh and L. Chen, Pre-treatment by combining atmospheric cold plasma and pH-shifting to prepare pea protein concentrate powders with improved gelling properties, *Food Res. Int.*, 2022, **154**, 111028.

19 X. Ge, H. Shen, C. Su, B. Zhang, Q. Zhang, H. Jiang, *et al.*, Improving effects of cold plasma on multi-scale structure, physicochemical and digestive properties of dry heated red adzuki bean starch, *Food Chem.*, 2021, **349**, 129159.

20 J. Wang, X. Zhou, J. Li, D. Pan and L. Du, Enhancing the functionalities of chickpea protein isolate through a combined strategy with pH-shifting and cold plasma treatment, *Innovative Food Sci. Emerging Technol.*, 2024, **93**, 103607.

21 J. Chu, F. Zhou, Z. Wu, W. Ouyang, Z. Ma, S. Liang, *et al.*, Atmospheric cold plasma treatment of peanut protein: structural and functional modifications accompanied by microbial reduction, *J. Food Eng.*, 2025, 112825.

22 W. Gong, X. Guo, H. Huang, X. Li, Y. Xu and J. Hu, Structural characterization of modified whey protein isolates using cold plasma treatment and its applications in emulsion oleogels, *Food Chem.*, 2021, **356**, 129703.

23 H. Ji, F. Han, S. Peng, J. Yu, L. Li, Y. Liu, *et al.*, Behavioral solubilization of peanut protein isolate by atmospheric

pressure cold plasma treatment, *Food Bioprocess Technol.*, 2019, **12**(12), 2018–2027.
24 P. André, J. Aubreton, M. F. Elchinger, P. Fauchais and A. Lefort, A modified pseudoequilibrium calculation to determine composition of hydrogen and nitrogen plasmas at atmospheric pressure, *Plasma Chem. Plasma Process.*, 2001, **21**(1), 83–105.
25 L. Xu, H. Hou, B. Farkas, K. M. Keener, A. L. Garner and B. Tao, High voltage atmospheric cold plasma modification of bovine serum albumin, *LWT*, 2021, **149**, 111995.
26 Y. Deng, Y. Lu, Y. Jiang, G. Yuan, T. Yang, B. Gao, *et al.*, Effect of cold plasma treatment time on walnut protein isolate: revealing structural changes and improving functional properties, *Int. J. Biol. Macromol.*, 2025, **311**, 143693.
27 X. Liu, F. Xue and B. Adhikari, Recent advances in plant protein modification: spotlight on hemp protein, *Sustainable Food Technol.*, 2024, **2**(4), 893–907.
28 H. Ji, S. Dong, F. Han, Y. Li, G. Chen, L. Li, *et al.*, Effects of dielectric barrier discharge cold plasma treatment on physicochemical and functional properties of peanut protein, *Food Bioprocess Technol.*, 2018, **11**(2), 344–354.
29 M. Sadat Hosseini, R. Farahmandfar, A. Motamedzadegan, N. Mollakhalili-Meybodi and W. F. Lai, Modifying the techno-functional characteristics of quinoa protein isolate by atmospheric cold plasma, *Food Hydrocolloids*, 2025, 111583.
30 M. Malik, H. Sharma and C. Saini, Effect of removal of phenolic compounds on structural and thermal properties of sunflower protein isolate, *J. Food Sci. Technol.*, 2016, **53**(9), 3455–3464.
31 A. Kheto, A. Mallik, R. Sehrawat, K. Gul and W. Routray, Atmospheric cold plasma-induced nutritional, anti-nutritional, molecular modifications and in vitro protein digestibility of guar seed flour, *Food Res. Int.*, 2023, **168**, 112790.
32 Y. Li, Y. Cheng, Z. Zhang, Y. Wang, B. K. Mintah, M. Dabbour, *et al.*, Modification of rapeseed protein by ultrasound-assisted pH shift treatment: ultrasonic mode and frequency screening, *Ultrason. Sonochem.*, 2020, **69**, 105240.
33 O. H. Lowry, N. J. Rosebrough, A. L. Farr and R. J. Randall, Protein measurement with the Folin phenol reagent, *J. Biol. Chem.*, 1951, **193**(1), 265–275.
34 M. A. Malik and C. S. Saini, Rheological and structural properties of protein isolates extracted from dephenolized sunflower meal: effect of high intensity ultrasound, *Food Hydrocolloids*, 2018, **81**, 229–241.
35 M. A. Malik and C. S. Saini, Polyphenol removal from sunflower seed and kernel: effect on functional and rheological properties of protein isolates, *Food Hydrocolloids*, 2017, **63**, 705–715.
36 E. Both, R. Boom and M. Schutyser, Particle morphology and powder properties during spray drying of maltodextrin and whey protein mixtures, *Powder Technol.*, 2020, **363**, 519–524.
37 A. Kheto, R. Sehrawat, K. Gul and L. Kumar, Effect of extraction pH on amino acids, nutritional, in vitro protein digestibility, and functional properties of guar germ proteins, *Food Chem.*, 2024, **444**, 138628.
38 C. S. Saini, H. K. Sharma and L. Sharma, Thermal, structural and rheological characterization of protein isolate from sesame meal, *J. Food Meas. Charact.*, 2018, **12**(1), 426–432.
39 Y. Chen, Y. Chen, L. Jiang, J. Wang and W. Zhang, Binding mechanism between coconut globulin and tannic acid mediated by atmospheric cold plasma, *Food Chem.*, 2025, **464**, 141670.
40 G. Eazhumalai, T. K. Ranjitha Gracy and U. S. Annapure, Cold plasma enhanced gelation and thermal properties of oat protein and applications in a model food system, *Sustainable Food Technol.*, 2025, **3**(4), 1203–1221.
41 L. Zhao, J. Zheng, W. Yan, J. Qian, J. Zhang, J. Wang, *et al.*, Cold plasma inhibited Aspergillus flavus and improved physicochemical properties of peanut protein, *Food Chem.*, 2025, **464**, 141607.
42 J. Wang, X. Zhou, S. Ju, R. Cai, M. Roopesh, D. Pan, *et al.*, Influence of atmospheric pressure plasma jet on structural and digestive properties of chickpea protein isolate, *Food Res. Int.*, 2023, **174**, 113565.
43 X. Zhang, B. Qi, F. Xie, M. Hu, Y. Sun, L. Han, *et al.*, Emulsion stability and dilatational rheology of soy/whey protein isolates at the oil–water interface: influence of pH, *Food Hydrocolloids*, 2021, **113**, 106391.
44 J. J. Yu, Z. Y. Zhang, X. N. Lin, Y. Q. Ji, R. R. Zhang, H. Ji, *et al.*, Cold plasma oxidation-induced changes in hydration and structure of high-temperature peanut protein, *Int. J. Biol. Macromol.*, 2023, **253**, 127500.
45 G. Eazhumalai, R. G. T. Kalaivendan and U. S. Annapure, Atmospheric pin-to-plate cold plasma effects on oat protein: structural, chemical and foaming characteristics, *Int. J. Biol. Macromol.*, 2023, **242**, 125103.
46 S. Dong, P. Guo, Y. Chen, G. Y. Chen, H. Ji, Y. Ran, *et al.*, Atmospheric cold plasma modification of zein: physicochemical and functional properties, *Ind. Crops Prod.*, 2018, **115**, 124–133.
47 H. An and H. Zheng, Correlations between powder functionalities and surface properties of milk protein ingredients, *J. Dairy Sci.*, 2025, **108**(1), 190–205.
48 M. Abarghoei, M. Goli and S. Shahi, Cold atmospheric plasma effects on functional and physicochemical properties of wheat germ protein isolate, *LWT*, 2023, **177**, 114585.
49 A. Dabade, S. Kahar, A. Acharjee and U. S. Annapure, Atmospheric cold plasma effects on structural and functional properties of soy protein isolate, *J. Agric. Food Res.*, 2023, **12**, 100538.
50 H. M. Mehr and A. Koocheki, Short- and long-term cold plasma effects on color, structure and Pickering foaming properties of grass pea protein, *Food Hydrocolloids*, 2023, **143**, 108846.
51 H. M. Mehr and A. Koocheki, Atmospheric cold plasma effects on structure, interfacial and emulsifying properties of grass pea protein isolate, *Food Hydrocolloids*, 2020, **106**, 105899.

52 L. Tan, X. Hua, L. Yin, X. Jia and H. Liu, Corona discharge cold plasma effects on structure and emulsification properties of soybean protein isolate, *Food Hydrocolloids*, 2024, **156**, 110337.
53 W. Ji, M. Li, T. Yang, H. Li, W. Li, J. Wang, *et al.*, Cold plasma effects on physical-biochemical properties and nutritional components of soybean sprouts, *Food Res. Int.*, 2021, **161**, 111766.
54 A. Ellis, A. Norton, T. Mills and I. Norton, Stabilisation of foams by agar gel particles, *Food Hydrocolloids*, 2017, **73**, 222–228.
55 Q. Li, F. Shen, X. He, C. Xing, W. Yan, Y. Fang, *et al.*, Modification of soy protein using dielectric barrier discharge cold plasma under modified atmosphere packaging, *Food Chem.*, 2023, **401**, 134158.
56 S. Rout and P. P. Srivastav, Modification of soy and pea protein isolates by high-voltage dielectric barrier discharge atmospheric cold plasma: comparative structural and functional study, *Food Chem.*, 2024, **447**, 138914.
57 S. Dhua, A. Kheto, V. S. Sharanagat, L. Singh, K. Kumar and P. K. Nema, Quality characteristics of roasted pigmented wheat, *Food Chem.*, 2021, **365**, 130372.
58 P. I. Haris and F. Severcan, FTIR spectroscopic characterization of protein structure in aqueous and non-aqueous media, *J. Mol. Catal. B: Enzym.*, 1999, **7**(1–4), 207–221.
59 K. Candoğan, E. G. Altuntas and N. İğci, Authentication and quality assessment of meat products by FTIR spectroscopy, *Food Eng. Rev.*, 2021, **13**(1), 66–91.
60 M. Manzoor, J. Singh and A. Gani, Structural and nutraceutical characterization of apple seed flour, *LWT*, 2021, **151**, 112138.
61 S. Yang, Q. Zhang, H. Yang, H. Shi, A. Dong, L. Wang, *et al.*, Progress in infrared spectroscopy as a tool for predicting protein secondary structure, *Int. J. Biol. Macromol.*, 2022, **206**, 175–187.
62 P. Guerrero, E. Beatty, J. Kerry and K. De la Caba, Extrusion of soy protein with gelatin and sugars at low moisture content, *J. Food Eng.*, 2012, **110**(1), 53–59.
63 P. Sahni, S. Sharma and V. K. R. Surasani, Processing and pH effects on alfalfa protein isolates: amino acids, morphology, electrophoresis, bioactivity and functionality, *Food Chem.*, 2020, **333**, 127503.
64 D. Das, P. S. Panesar and C. S. Saini, pH-shifting treatment of ultrasonically extracted soybean meal protein isolate, *Process Biochem.*, 2022, **120**, 227–238.
65 X. Zhao, H. Zhu, J. Chen and Q. Ao, FTIR, XRD and SEM analysis of ginger powders of different size, *J. Food Process. Preserv.*, 2015, **39**(6), 2017–2026.
66 S. Yadav, S. Mishra and R. C. Pradhan, Ultrasound-assisted hydration of finger millet and its effects on starch isolates and antinutrients, *Ultrason. Sonochem.*, 2021, **73**, 105542.
67 E. Bormashenko, Y. Bormashenko, I. Legchenkova and N. M. Eren, Cold plasma hydrophilization of soy protein isolate and milk protein concentrate for surfactant-free suspensions, *Innovative Food Sci. Emerging Technol.*, 2021, **72**, 102759.
68 M. Jahromi, M. Niakousari, M. T. Golmakani, F. Ajalloueian and M. Khalesi, Atmospheric cold plasma effects on structural and techno-functional properties of sodium caseinate, *Innovative Food Sci. Emerging Technol.*, 2020, **66**, 102542.
69 J. Luo, M. M. Nasiru, W. Yan, H. Zhuang, G. Zhou and J. Zhang, Structural and binding capacity changes of myofibrillar proteins from cold plasma-treated bacon, *LWT*, 2020, **117**, 108606.
70 S. Dong, A. Gao, Y. Zhao, Y. T. Li and Y. Chen, Physicochemical and structural properties of atmospheric cold plasma-modified zein, *Food Bioprod. Process.*, 2017, **106**, 65–74.
71 D. B. Choudhury, K. Subrahmanyam, S. Sahoo, K. Gul, R. Sehrawat and R. Y. Gan, In-package cold plasma tailoring molecular, structural and interfacial properties of soy protein isolate for stabilizing Pickering emulsions, *Innovative Food Sci. Emerging Technol.*, 2025, 104079.
72 A. Rezvankhah, M. S. Yarmand, B. Ghanbarzadeh and H. Mirzaee, Bioactive peptides from lentil protein: degree of hydrolysis, antioxidant activity, phenols, ACE-inhibition, sensory and functionality, *J. Food Meas. Charact.*, 2021, **15**(6), 5021–5035.
73 P. Liu, H. Xu, Y. Zhao and Y. Yang, Rheological properties of soy protein isolate solution for fibers and films, *Food Hydrocolloids*, 2017, **64**, 149–156.
74 P. Liu, H. Xu, Y. Zhao and Y. Yang, Rheological properties of soy protein isolate solution for fibers and films, *Food Hydrocolloids*, 2017, **64**, 149–156.
75 M. M. Rahman and B. P. Lamsal, Cold plasma and high-power sonication effects on rheological and gelling properties of mung bean protein, *Food Res. Int.*, 2023, **163**, 112265.
76 H. M. Moreno, F. Dominguez-Timon, M. T. Díaz, M. M. Pedrosa, A. J. Borderías and C. A. Tovar, Gels made with commercial pea protein isolate: rheological, structural and functional evaluation, *Food Hydrocolloids*, 2020, **99**, 105375.
77 A. Acharjee, A. Dabade, S. Kahar and U. S. Annapure, Atmospheric cold plasma effects on structural and functional properties of pea protein isolate, *J. Agric. Food Res.*, 2023, **14**, 100821.